Digital Object Identifier (DOI): 10.1109/APEC.2013.6520316

IEEE Press

## Harmonics Suppression for Single-Phase Grid-Connected Photovoltaic Systems in Different Operation Modes

Yongheng Yang
Keliang Zhou
Frede Blaabjerg

## Suggested Citation

Yang, Y., Zhou, K. & Blaabjerg, F. , ”Harmonics Suppression for Single-Phase Grid-Connected Photovoltaic Systems in Different Operation Modes,” 2013 Proceedings of the IEEE Applied Power Electronics Conference and Exposition, 2013. IEEE Press, s. 889-896 8 s.

# Harmonics Suppression for Single-Phase Grid-Connected PV Systems in Different Operation Modes

Yongheng Yang[1], Keliang Zhou[2], Frede Blaabjerg[1]

[1]Department of Energy Technology
Aalborg University
Pontoppidanstraede 101, Aalborg DK-9220, Denmark
yoy@et.aau.dk, fbl@et.aau.dk

[2]Department of Electrical and Computer Engineering
University of Canterbury
Private Bag 4800, Christchurch 8020, New Zealand
eklzhou@ieee.org

***Abstract*- As the penetration of grid-connected photovoltaic (PV) systems is booming, specific grid demands are imposed on such interconnected PV systems. Therefore, achieving high reliable PV systems with high power quality is of intense interest. However, the injected current from single-phase grid-connected PV inverters may be severely affected in different operation modes. In this paper, a detailed analysis is conducted to reveal the relationship between the harmonics level with the power factor and the current level in the PV systems. A current control solution which employs an Internal Model Principle (IMP) is proposed to suppress the harmonic currents injected into the grid. Experiments are carried out to verify the analysis and the performance of the proposed control method. It is demonstrated that the proposed method presents an effective solution to harmonics suppression for single-phase grid-connected PV systems in different operation modes. Especially, it can remove higher order harmonics effectively leading to a better power quality compared to the Proportional plus Multi-Resonant Controller, and it has less computational burden.**

## I. INTRODUCTION

Recently, the penetration of single-phase grid-connected PV systems is increasing progressively mainly due to the matured PV technology and the declined PV module price [1]. This intense integration into the grid also causes challenges the availability, power quality and emerging reliability of the entire PV system. Consequently, specific grid requirements are expected to be strengthened to regulate the grid-connected PV systems. In the future, the single-phase grid-connected PV system will be more active in different operation modes and provide low voltage ride through (LVRT) capability and grid support function in the presence of a grid fault. However, this might degrade the power quality with the risk of introducing resonances. The control system should maintain the power quality under both normal operation and in low voltage ride through operation to meet the existing or upcoming grid requirements [2]-[4]. For example, it is stated in IEEE 929 standard that the Total Harmonic Distortion (THD) for the grid current should be lower than 5% in normal operation [4].

In order to eliminate the current distortion, many current control methods are proposed [2], [5]-[11], [14]. For instance, in [6], the Proportional Resonant (PR) controller and Multi-Resonant Controllers (MRC) are developed and their performances are much better than the conventional Proportional Integrator (PI) controller. However, it introduces computational burden particularly when high-order harmonics, e.g. the $11^{th}$ and $13^{th}$ order harmonics, are required to be compensated. Repetitive current controller, which is based on Internal Model Principle (IMP), is implemented in [8], [11] with satisfactory tracking accuracy, but it presents a slower dynamic performance and its stability range is typically not wide enough [18]. Moreover, even with advanced control schemes to regulate the injected current from the single-phase grid-connected PV systems, it is found that the even order voltage harmonic ripples at the DC side (PV panels) may still distort the injected current, leading to a poor current THD. Meanwhile, it can also be summarized from the test data that the harmonic current level varies with the injected current level and the power factor.

With the increasing penetration of grid-connected PV power systems, the grid requirements will be more stringent in the future in terms of the power quality. Since the causes of the harmonic current injection from the single-phase grid-connected PV inverters are not well investigated in different operation modes, there is no good guideline about how to develop an appropriate control system to guarantee a proper power quality of the injected current under such conditions. For example, when the system operates at non-unity power factor in LVRT mode to provide an amount of reactive power, the injected current may be severely affected, which may lead to the instability of the entire system. Therefore, it is necessary to investigate this relationship.

In this paper, the mechanism of the harmonic current injection from the single-phase grid-connected PV systems is studied. In particular, the relationship between the current power quality and the power factor and the current level under different operation modes is analyzed. Based on these discussions, a current control solution is proposed to suppress the current harmonics. Finally, the proposed control method is validated by a 1 kW single-phase grid-connected system in order to test the effectiveness of the proposed control method.

## II. MECHANISM OF HARMONIC CURRENT INJECTION

### A. Problem Description

A grid-connected single-phase PV system based on a single-phase *PQ* theory control method [5], [13] is shown in Fig. 1. It also shows a sag generator, which functions by switching the resistance $R_s$ and $R_L$ to simulate a grid fault. By adjusting the active power and reactive power references ($P^*$, $Q^*$), the power factor can be controlled.

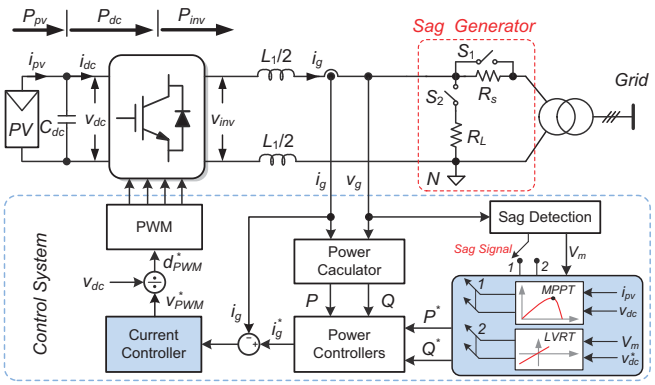


Fig. 1. Overall control structure of a single-phase grid-connected PV system based on the single-phase *PQ* theory (1: normal MPPT operation; 2: low voltage ride through operation).

As it is stated previously, the single-phase grid-connected PV system should fulfill the requirements in different operation modes in order to maintain the quality, stability and reliability of the entire system. Similar to the conventional power plants, the PV systems are expected to support the grid by means of injecting reactive power into the grid in the presence of a voltage drop. Consequently, the power factor is not unity anymore and the power quality is affected.

According to the grid support requirement defined for wind power systems by E.ON [26], the current injected into the grid during low voltage ride through can be given as [5],

$$I_q = \begin{cases} \text{over-voltage}, & V \geq 1.1 p.u. \\ \text{normal operation}, & 0.9 p.u. \leq V < 1.1 p.u. \\ k \cdot \dfrac{V - V_0}{V_N} \cdot I_N + I_{q0}, & 0.5 p.u. \leq V < 0.9 p.u. \\ -I_N + I_{q0}, & V < 0.5 p.u. \end{cases}, \quad (1)$$

where,

$V$, $V_0$, and $V_N$ are the amplitudes of the instantaneous grid voltage, initial voltage before grid faults and the nominal grid voltage,

$I_q$, $I_{q0}$, and $I_N$ are the required current, the initial reactive current before a grid failure and the nominal current, and

$k = (\Delta I_q / I_n)/(\Delta V / V_n) \geq 2$ p.u., $\Delta I_q = I_q - I_{q0}$, $\Delta V = V - V_0$.

Normally, before the grid failure, the grid voltage $V_0 = V_N$ and the system is operating at unity power factor, which means $I_{q0} = 0$ A. Thus, according to (1), the power factor, cos$\varphi$, in the different operation modes can be given by,

$$\cos\varphi = \frac{P}{\sqrt{P^2 + Q^2}} = \begin{cases} 1, & 0.9 p.u. \leq V < 1.1 p.u. \\ \sqrt{1 - k^2 \cdot \left( \dfrac{V - V_0}{V_N} \right)^2}, & 0.5 p.u. \leq V < 0.9 p.u. \\ 0, & V < 0.5 p.u. \end{cases}, \quad (2)$$

in which $k$ is defined previously. It is shown in (2) that by regulating the active power $P$ and reactive power $Q$ shown in Fig. 1, the grid current reference $i^*_g$ with the desirable power factor can be generated. This relationship between the power factor and the voltage sag depth under different $k$ can be plotted as shown in Fig. 2.

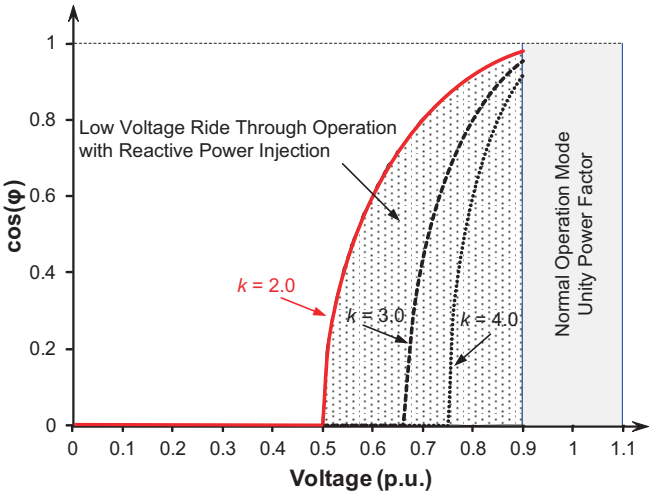


Fig. 2. Power factor curve under different voltage sag depths according to the E.ON grid code defined for wind power systems.

It is shown in Fig. 2 that during low voltage ride through the power factor is changed with the voltage sag depth, which may affect the power quality. Previous experimental results using the proportional resonant controller which are shown in Fig. 3 also demonstrated that both the power angle $\varphi$ and the current level have a significant impact on the average THD of the injected current. Therefore, in the low voltage ride through operation mode, the injected current might be distorted and it is necessary to investigate this relationship in order to design an appropriate control scheme.

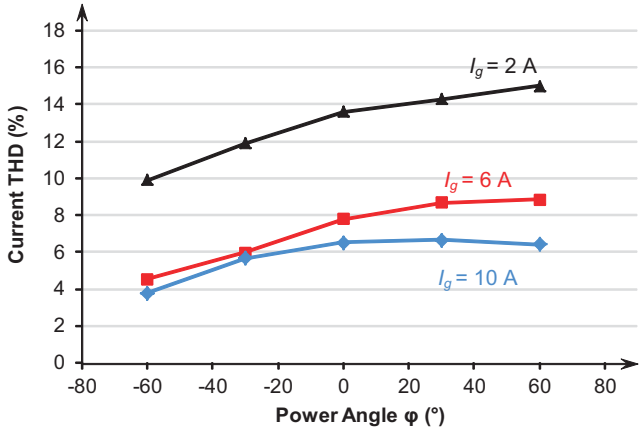


Fig. 3. Measured grid current THD vs. power angle for a single-phase grid-connected system under different current levels in normal operation using proportional resonant current control method.

## B. *Mechanism of Harmonic Current Injection*

The system shown in Fig. 1 can be described by,

$$L_1 \frac{di_g}{dt} = v_{inv} - v_g, \quad (3)$$

$$i_{dc} = i_{pv} - C_{dc}\frac{dv_{dc}}{dt}, \tag{4}$$

where $v_{inv}$ is the PV inverter output voltage, $v_g$ is the grid voltage and $L_1$ is the inverter-side filter.

It is seen from (3) that if $v_{inv}$ or/and $v_g$ contains any harmonics, it will propagate to the injected grid current $i_g$, leading to a poorer THD. The grid current can be written as,

$$i_g = \frac{1}{L_1}\int\left\{\left(v_{inv1} + \sum_2^n v_{invi}\right) - \left(v_{g1} + \sum_2^n v_{gi}\right)\right\}, \tag{5}$$

$$i_g = i_{g1} + \sum_{i=2}^{n}\tilde{i}_{Ci} - \sum_{i=2}^{n}\tilde{i}_{Gi} = i_{g1} + \sum_{i=2}^{n} i_{gi}, \tag{6}$$

in which,

$v_{inv1}$ and $v_{invi}$ are the fundamental frequency component and the $i$-th harmonic component of the output voltage $v_{inv}$,

$v_{g1}$ and $v_{gi}$ are the fundamental frequency component and the $i$-th harmonic component of the grid voltage $v_g$,

$i_{g1}$ is the fundamental frequency component of $i_g$, and

$\tilde{i}_{Ci}$ and $\tilde{i}_{Gi}$ are the $i$-th current harmonic of the grid current $i_g$ caused by the harmonic components of the inverter output voltage $v_{inv}$ and the grid voltage $v_g$ respectively.

It is also implied in (5) and (6) that the current harmonics $\tilde{i}_{Gi}$ in the injected current $i_g$ can be eliminated by the inverter output voltage $v_{inv}$ if an appropriate control method is applied to the grid-connected PV inverter.

Given that the grid voltage quality is good enough, the harmonics distortion induced by the grid voltage distortion could be ignored. Since the harmonics induced by the PV inverters are dominant in the injected current, the following discussion is done firstly by considering of $\tilde{i}_{Ci}$. By neglecting the high switching frequency harmonics (or they can be filtered out by means of an $LC$-filter), the PV inverter output voltage $v_{inv}$ can be written as,

$$\begin{aligned} v_{inv} &= d_{PWM}v_{dc} = \left(d_{PWM1} + \tilde{d}_{PWM}\right)\left(V_{dc} + \tilde{v}_{dc}\right) \\ &= d_{PWM1}V_{dc} + d_{PWM1}\tilde{v}_{dc} + V_{dc}\tilde{d}_{PWM} + \tilde{v}_{dc}\tilde{d}_{PWM}, \\ &= v_{inv1} + \sum_{i=2}^{n} v_{invi} \end{aligned} \tag{7}$$

where,

$d_{PWM}$ is the output of the current controller and the input to the PWM modulator and $-1 \le d_{PWM} \le 1$, $d_{PWM1}$ and $\tilde{d}_{PWM}$ are the fundamental frequency component and harmonic components of $d_{PWM}$,

$V_{dc}$ and $\tilde{v}_{dc}$ are the DC and AC components of the voltage $v_{dc}$ across the DC power decoupling capacitor $C_{dc}$.

This equation demonstrates that the voltage harmonics $v_{invi}$ is induced by the PWM harmonics, $\tilde{d}_{PWM}$, and the voltage variation, $\tilde{v}_{dc}$, across the DC capacitor. Consequently, such impact will propagate to the injected current and affect the power quality. Here, the high order component, $\tilde{v}_{dc}\tilde{d}_{PWM}$, is ignored for simplicity.

Let the fundamental grid voltage $v_{g1}=\sqrt{2}V_{g1}\cos(\omega_0 t+\varphi)$, the fundamental injected grid current $i_{g1}=\sqrt{2}I_{g1}\cos(\omega_0 t)$ and the inverter output voltage $v_{inv1}=\sqrt{2}V_{inv1}\cos(\omega_0 t+\varphi-\varphi_1)$ for the following discussion. According to Fig. 1, the DC side instantaneous power $p_{dc}$ which is the input power of the PV inverter and the inverter output instantaneous power $p_{inv}$ can be expressed as,

$$\begin{cases} p_{dc} = v_{dc}i_{PV} - v_{dc}C_{dc}\dfrac{dv_{dc}}{dt} \\ \quad = v_{dc}i_{PV} - C_{dc}V_{dc}\dfrac{d\tilde{v}_{dc}}{dt} - \dfrac{C_{dc}}{2}\dfrac{d\tilde{v}_{dc}^2}{dt}, \\ p_{inv} = V_{inv1}I_{g1}\cos(\varphi-\varphi_1) + V_{inv1}I_{g1}\cos(2\omega_0 t+\varphi-\varphi_1) \\ \quad + \left(i_{g1}\sum_{i=2}^{n} v_{invi} + v_{inv1}\sum_{i=2}^{n} i_{gi}\right). \end{cases} \tag{8}$$

where $\omega_0$ is the grid fundamental frequency and $\varphi$ is the power angle.

Neglecting the PV inverter losses, $p_{inv}=p_{dc}$, and $p_{pv}=v_{dc}i_{PV} \approx V_{inv1}I_{g1}\cos(\varphi-\varphi_1)$. Since $|V_{dc}| \gg |\tilde{v}_{dc}|$, $|i_{g1}| \gg |i_{gi}|$ and $|v_{inv1}| \gg |v_{invi}|$ in most cases and the second order component $d\tilde{v}_{dc}^2/dt$ in the DC side instantaneous power $p_{dc}$ can be ignored, the following equation can be obtained from (8),

$$\tilde{v}_{dc} \approx -\int\left(\frac{V_{inv1}I_{g1}}{C_{dc}V_{dc}}\cos(2\omega_0 t+\varphi-\varphi_1)\right)dt. \tag{9}$$

This relationship reveals that the amplitude of the variation at the DC side $|\tilde{v}_{dc}|$ is proportional to the inverter output voltage level $V_{inv1}$ and the grid current level $I_{g1}$. This can also be illustrated by the phasor diagram shown in Fig. 4. It can be seen in Fig. 4 that the length of the inverter output voltage $\vec{v}_{inv1}$ changes with the phase angle $\varphi$, e.g. $\vec{v}_{inv1}$ reaches its maximum length at $\varphi = 90°$, while the minimum length at $\varphi = -90°$ assuming that the output filter $L_1$ is mainly inductive.

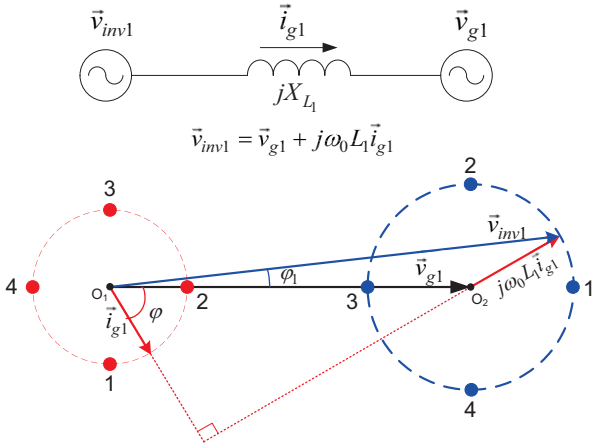


Fig. 4. Simplified model and the phasor diagram of the AC side circuit shown in Fig. 1 (only fundamental components).

According to (7), it can be concluded that the variation $|\tilde{v}_{dc}|$ at the DC capacitor $C_{dc}$ will introduce harmonics in the inverter output voltage $v_{inv}$. This impact will pass to the injected current and deteriorate the current quality as it is

seen from (5) and (6). This explains why under different power angle the average THDs shown in Fig. 3 are variable. Moreover, it is shown in (9) that $\tilde{v}_{dc}$ mainly comprises of even harmonics with a frequency of $2k\omega_0$ ($k$ =1, 2, 3, …). Consequently, $d_{PWMI}\tilde{v}_{dc}$ will produce odd harmonics with the frequency of $(2k+1)\omega_0$, $k$ =1, 2, …. It will inherently inject odd current harmonics because both $d_{PWMI}$ and $\tilde{v}_{dc}$ are unavoidable elements in a closed-loop control for a grid-connected PV inverter.

It is also seen from (7) that $V_{dc}\tilde{d}_{PWM}$ can be used to eliminate the harmonics caused by $d_{PWMI}\tilde{v}_{dc}$ if the inverter controller is appropriately designed; otherwise $V_{dc}\tilde{d}_{PWM}$ may even worsen the injected current harmonics level.

When a grid voltage drop happens, the power quality of the injected current will be affected by the voltage sag. The instantaneous inverter output power can also be expressed as,

$$\begin{aligned} p_{inv} &= \left(v_g + L_1\frac{di_g}{dt}\right)i_g \\ &\approx V_{g1}I_{g1}\cos\varphi + V_{g1}I_{g1}\cos\left(2\omega_0 t+\varphi\right) \\ &\quad -\omega_0 L_1 I_{g1}^2\sin\left(2\omega_0 t\right)+\left(i_{g1}\sum_{i=2}^{n}v_{gi}+v_{g1}\sum_{i=2}^{n}i_{gi}\right) \end{aligned} \quad (10)$$

Similarly, ignoring the inverter power losses and the higher order components, the following is valid,

$$C_{dc}V_{dc}\frac{d\tilde{v}_{dc}}{dt} \approx V_{g1}I_{g1}\cos\left(2\omega_0 t+\varphi\right)-\omega_0 L_1 I_{g1}^2\sin\left(2\omega_0 t\right), \quad (11)$$

and,

$$\tilde{v}_{dc} \approx -\int\left(\frac{V_{g1}I_{g1}}{C_{dc}V_{dc}}\cos\left(2\omega_0 t+\varphi\right)-\frac{\omega_0 L_1 I_{g1}^2}{C_{dc}V_{dc}}\sin\left(2\omega_0 t\right)\right)dt. \quad (12)$$

Equation (12) implies that the voltage variation across the DC capacitor is proportional to the grid voltage amplitude. Therefore, in low voltage ride through operation mode, the variation is smaller than in the normal operation. Based on the phasor diagrams shown in Fig. 5, it can be predicted that the power quality will be better in low voltage ride through operation mode if the grid current is kept the same as it is in the normal condition.

All above analysis elaborates the mechanism of harmonic current injection of a single-phase grid-connected PV system in different operation modes. This mechanism can be used to develop appropriate control methods in order to suppress the harmonic current injections from the PV inverters.

## III. Harmonics Suppression Control

### A. Proposed Harmonics Control Method

If the reference $i_g^*$ shown in Fig. 1 is a pure sinusoidal signal at the grid fundamental frequency and the gains of the current controller at the harmonic frequencies are high enough, the injected harmonics will be suppressed in steady state. Based on the Internal Model Principle (IPM), a Proportional Resonant (PR) [3], [6], [7], [21]-[24] plus Repetitive Current (RC) [8]-[12], [14]-0 controller (PR+RC) is proposed to eliminate harmonic current injection, as it is shown in Fig. 6.

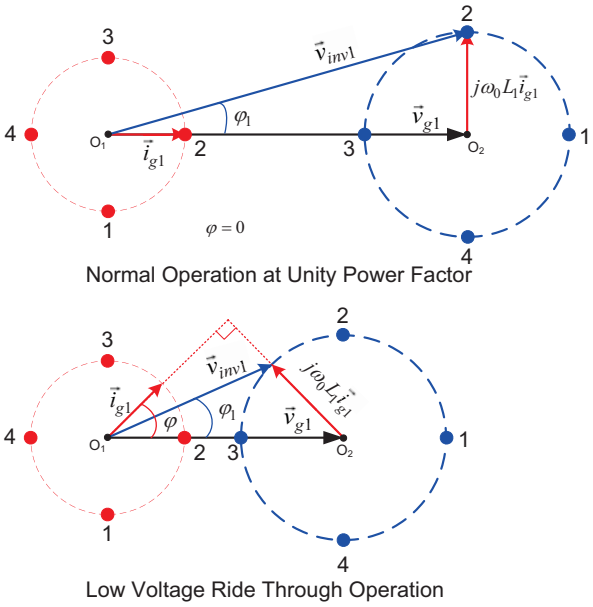


Fig. 5. Phasor diagrams for a single-phase grid-connected PV system in different operation modes.

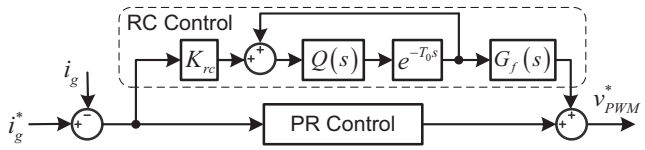


Fig. 6. Proposed current control scheme based on internal model principle.

This current control method is designed to suppress the harmonic distortions caused by $u_g$ and $d_{PWMI}\tilde{v}_{dc}$. Note that, although RC can suppress all harmonics below the Nyquist frequency, the response of the repetitive controller is very slow in removing high order harmonics due to its fundamental period time-delay. Multi-Resonant Controllers (MRC), which connects the resonant controllers in parallel for each harmonic, can eliminate major harmonic distortions at a much faster speed. However, it is at the expense of heavy paralleling computation duty of the micro-controller. Moreover, when higher order harmonics (above the 11th and/or 13th order harmonics) need to be compensated, the MRC method will make the system to become unstable and it is less practical [18]. In this control structure, the PR controller is designed as a zero-tracking-error controller at the grid fundamental frequency and the RC controllers are designed to remove the harmonic components. The combination of PR and RC shown in Fig. 6 can make an optimal trade-off between control performance and practical realization.

### B. Controller Design

In the control scheme shown in Fig. 6, the transfer-function for the repetitive controller $G_{RC}(s)$ and the transfer-function for the PR controller $G_{PR}(s)$ can be expressed as,

$$G_{RC}\left(s\right)=\frac{K_{rc}e^{-T_0 s}Q\left(s\right)}{1-e^{-T_0 s}Q\left(s\right)}G_f\left(s\right), \quad (13)$$

$$G_{PR}(s) = K_P + K_R \frac{s}{s^2 + \omega_0^2}, \tag{14}$$

in which $K_{rc}$, $K_P$, and $K_R$ are the controller constants, $Q(s)$ is a low-pass filter for enhancing the stability of the repetitive control system and $G_f(s)=e^{Ts}$ provides a phase-lead compensation as discussed in [15], [18], with $T$ being the period of the phase-lead compensation, and $T_0$ is the fundamental period of the grid voltage.

In the discrete-time domain, the repetitive controller can also be expressed as,

$$G_{RC}(z) = \frac{K_{rc} z^{-N} Q(z)}{1 - z^{-N} Q(z)} G_f(z), \tag{15}$$

where $N = f_s/f_g$ with $f_s$ being the sampling frequency and $f_g$ being the grid fundamental frequency. For a zero phase compensation repetitive controller, the control gain $K_{rc}$ which determines the stability range of the control system is typically given by [8],

$$0 < K_{rc} < 2. \tag{16}$$

Due to the uncertainties, like computational delay, inaccurate high frequency characteristics of the plant and parameter variations, the zero-tracking-error cannot be achieved in steady state. To overcome this drawback, the low-pass filter $Q(z)$ is introduced to enhance the robustness of the controller and at the cost of tracking accuracy [8], [11], [18]. Usually, it can be chosen as [8],

$$Q(z) = \alpha_1 z + \alpha_0 + \alpha_1 z^{-1}, \tag{17}$$

in the discrete-time domain, where,

$$2\alpha_1 + \alpha_0 = 1, \quad \alpha_0, \alpha_1 > 0.$$

Moreover, $G_f(z)=z^m$ is used to compensate the un-modeled delays in the system [8], and the value of the phase-lead number $m$ is determined by experiments.

Hereafter, the closed-loop control scheme can be structured as shown in Fig. 7, where $G_p(s)$, $G_q(s)$ are the PI controllers for the active power and reactive power respectively, and $v_{g\alpha}$, $v_{g\beta}$ are the $\alpha\beta$ components of the grid voltage generated by a second-order generalized integrator based orthogonal generation system [2], [3], [5].

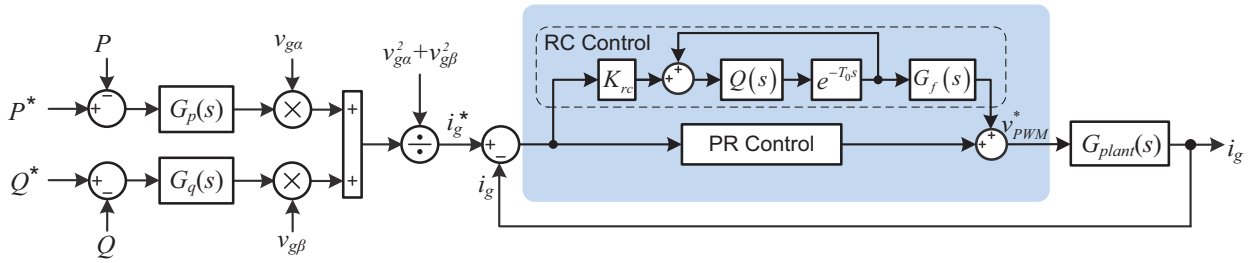


Fig. 7. Closed-loop control scheme for a single-phase grid-connected system based on the single-phase *PQ* theory [5], [13] and the proposed current harmonics suppression method.

## IV. Experimental Results

In order to verify the above analysis and to evaluate the proposed current control scheme, referring to Fig. 1, a single-phase grid-connected system is tested in the Green Power Lab at Aalborg University and the setup is shown in Fig. 8.

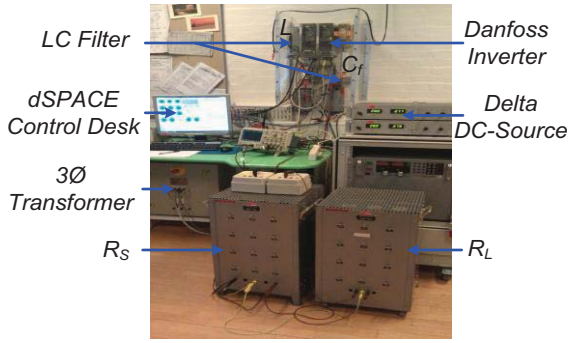


Fig. 8. Experimental setup of a single-phase grid-connected system.

In this application, a Danfoss three-phase 5 kW VLT inverter is used and it is configured as a single-phase system which is connected to the grid through a three-phase transformer. The control system is implemented in a DS 1103 dSPACE system. An *LC*-filter is employed in order to filter out the harmonics at high switching frequencies. The other control parameters for this test are listed in TABLE I. The experimental results are shown in Fig. 9, Fig. 10 and Fig. 11.

TABLE I

Parameters for the Experimental Validations

| | |
|---|---|
| Grid Voltage Amplitude | $V_g = 325\ V$ |
| Grid Frequency | $\omega_0 = 2\pi \times 50\ rad/s$ |
| *LC* Filter | $L_1 = 3.6\ mH$, $C_f = 2.35\ \mu F$ |
| PI parameters for $G_p(s)$ | $K_{pp}=1.2$, $K_{pi}=52$ |
| PI parameters for $G_q(s)$ | $K_{qp}=1$, $K_{qi}=50$ |
| Repetitive Controller Parameter | $K_{rc}=1.8$ |
| PR Controller Parameters | $K_P=22$, $K_R=2000$ |
| MRC Controller Parameters | $K_{i3}=5000$, $K_{i5}=5000$, $K_{i7}=7000$ (the 3rd, 5th and 7th harmonics are compensated) |
| Phase-lead Compensation Number | $m=4$ |
| Transformer Leakage Inductance and Resistance | $L_g = 4\ mH$, $R_g = 0.02\ \Omega$ |
| Sampling and Switching Frequency | $f_s = f_{sw} = 10\ kHz$ |

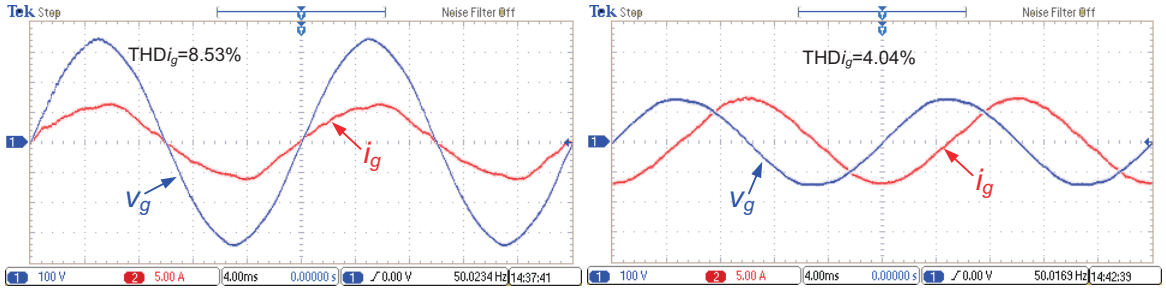


(a) normal operation (unity power factor, cosφ = 1) (b) low voltage ride through operation (0.5 p.u. voltage sag, cosφ = 0)

Fig. 9. Experimental results for a single-phase grid-connected system in different operation modes with proportional resonant control method: 1. grid voltage [$v_g$: 100 V/div]; 2. grid current [$i_g$: 5 A/div]; [$t$ = 4 ms/div].

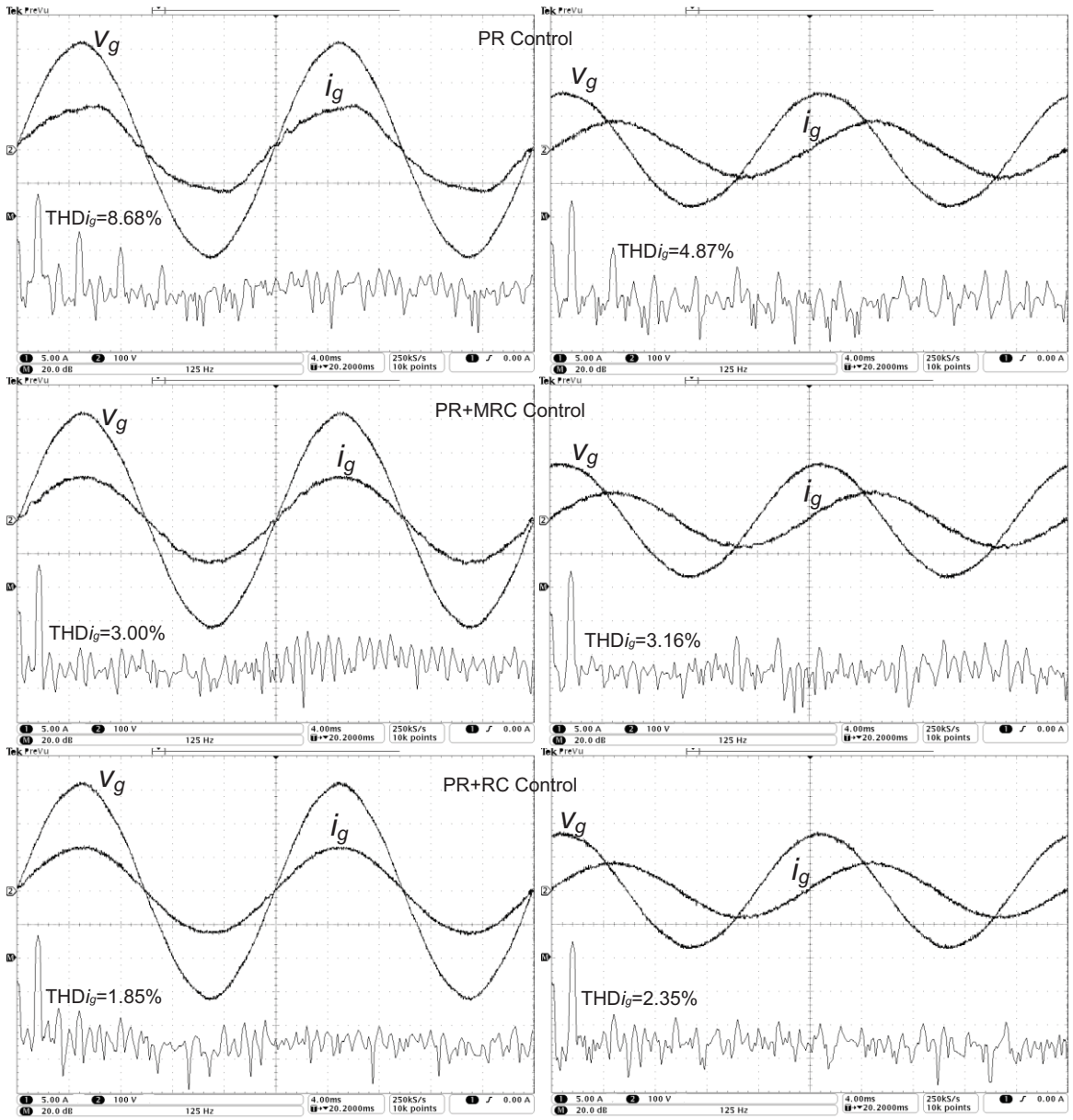


(a) normal operation (unity power factor) (b) low voltage ride through operation (0.45 p.u. voltage sag)

Fig. 10. Experimental results of a single-phase grid-connected system in different operation conditions with various current control methods based on the single-phase *PQ* theory: 1. grid current [$i_g$: 5 A/div]; 2. grid voltage [$v_g$: 100 V/div]; [$t$ = 4 ms/div]; [$f_{FFT}$ = 125 Hz/div].

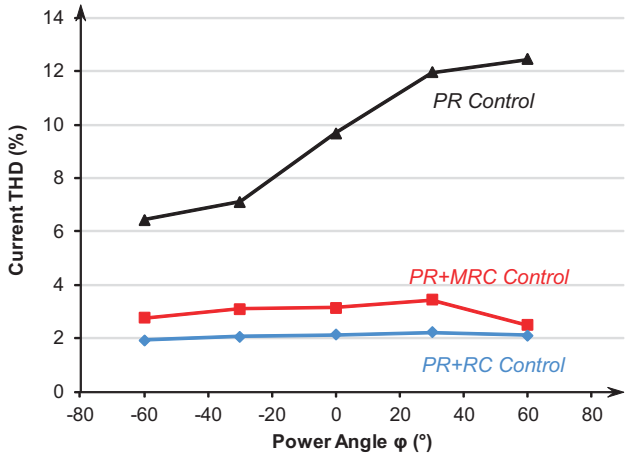


Fig. 11. Measured grid current THD vs. power angle for a single-phase grid-connected system under $I_g = 6$ A and $V_g = 230$ V in normal operation using various current control methods.

A voltage sag (0.45 p.u.) is generated by switching the resistors, $R_s$ and $R_L$ (see Fig. 2). During the grid fault, the system is injecting reactive power and limiting active power output in such a way that it prevents the inverter from overcurrent, which means that the power factor is not unity anymore. As it is shown in Fig. 9, the current THD is lower in the LVRT operation than in normal operation with unity power factor, which validates that the current THD varies with the power factor and is coincide with the above analysis. Moreover, it is also proved in Fig. 10 and Fig. 11 that the proposed control method can suppress the harmonics effectively. Compared to the PR+MRC method, the proposed PR+RC scheme has a better current quality both in normal operation and in low voltage ride through operation with a non-unity power factor, since it can remove high order harmonics effectively as it is proved by the FFT waveforms in Fig. 10. Furthermore, it has less computational burden when it is implemented in a digital signal processor in contrast with the PR+MRC method.

Fig. 12 and Fig. 13 show the Fast Fourier Transform of the injected current when the system is operating in the different modes using the PR+MRC and PR+RC current harmonics suppression methods. Since the 3rd-, 5th-, and 7th-order harmonics are compensated in the PR+MRC control scheme, such low-order harmonics are lower compared to those in the PR+RC control scheme; while the PR+RC control method presents an effective way to high-order harmonics suppression.

It should be pointed out that because the very low voltage operation as low voltage ride through mode is a short period, the transient behavior of the PR+RC might be worse than that of the PR+MRC. The transient performance can be improved by means of introducing phase compensation and optimizing the control gain $K_{rc}$ [15], [18]. Nevertheless, the performance of the PR+RC is better in steady state.

## V. Conclusions

This paper presents the mechanism of current harmonics injection in single-phase grid-connected PV systems in different operation modes. The analysis reveals how the

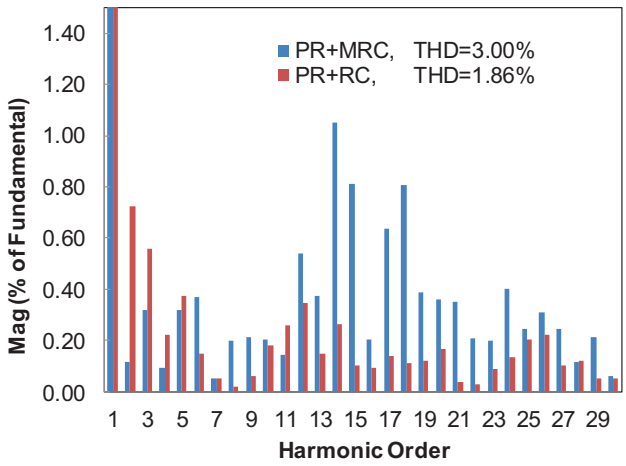


Fig. 12. FFT of the grid current for a single-phase grid-connected system in normal operation using different current control methods.

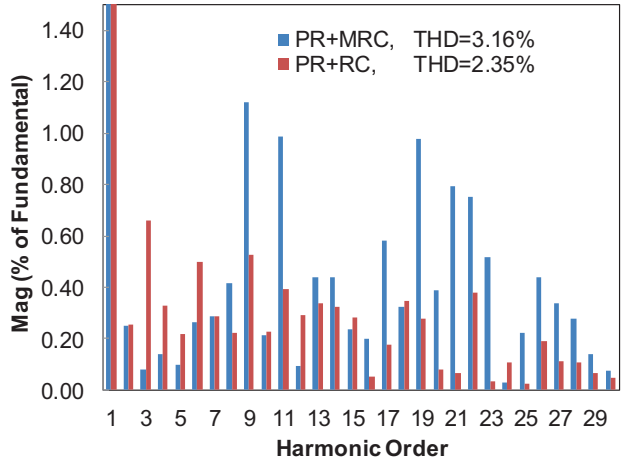


Fig. 13. FFT of the grid current for a single-phase grid-connected system in low voltage ride through operation (0.45 p.u. voltage sag) using different current control methods.

injected current distortion varies with the current level, the power factor and the grid voltage level during low voltage ride-through operation. The proposed method is designed based on this mechanism and it can suppress the injected harmonics effectively compared to a traditional proportional resonant controller. It can be concluded that the low order harmonics are dominant in the injected current. The proposed current control method and the PR plus multiple resonant controllers can be adopted to eliminate the harmonic injection. A comparison between PR+MRC and the proposed method demonstrates that the proposed control method (PR+RC) has a better performance in removing the high-order harmonic components in the injected current. It can be implemented in a digital signal processor with less computational burden when it is compared to PR+MRC method.

## Acknowledgment

The authors would like to give special thanks to China Scholarship Council (CSC) for supporting this PhD project in the Department of Energy Technology at Aalborg University, Denmark. The authors also would like to thank Assoc. Prof. Tamas Kerekes at Aalborg University for his help with the experimental setup.

## REFERENCES


[1] REN21, "Renewables Global Status Report 2012" [Online], Jun. 2012. Available: http://www.map.ren21.net/GSR/GSR2012.pdf.

[2] F. Blaabjerg, R. Teodorescu, M. Liserre, and A.V. Timbus, "Overview of control and grid synchronization for distributed power generation systems," *IEEE Trans. Ind. Electron.*, vol.53, no.5, pp.1398-1409, Oct. 2006.

[3] R. Teodorescu, M. Liserre, and P. Rodriguez, *Grid Converters for Photovoltaic and Wind Power Systems*, John Wiley & Sons, 2011.

[4] K. Zhou, Z. Qiu, Y. Yang, "Current harmonics suppression of single-phase PWM rectifiers," in *Proc. of PEDG'12*, pp.54-57, Jun. 2012.

[5] Y. Yang, F. Blaabjerg, and Z. Zou, "Benchmarking of grid fault modes in single-phase grid-connected photovoltaic systems," in *Proc. of ECCE*, pp. 4370-4377, 15-20 Sept. 2012.

[6] R. Teodorescu, F. Blaabjerg, M. Liserre, and P.C. Loh, "Proportional-resonant controllers and filters for grid-connected voltage-source converters," *IEE Proc.-Electr. Power Appl*, vol.153, no.5, pp.750-762, Sept. 2006.

[7] R. Teodorescu, F. Blaabjerg, U. Borup, and M. Liserre, "A new control structure for grid-connected LCL PV inverters with zero steady-state error and selective harmonic compensation," in *Proc. of APEC '04,* vol.1, pp. 580- 586, 2004.

[8] K. Zhou, K.-S. Low, D. Wang, F.L. Luo, B. Zhang, and Y. Wang, "Zero-phase odd-harmonic repetitive controller for a single-phase PWM inverter," *IEEE Trans. Power Electron.,*, vol.21, no.1, pp. 193- 201, Jan. 2006.

[9] T. Hornik and Q-C Zhong, "A current control strategy for voltage-source inverters in microgrids based on H-infinity and repetitive control, " *IEEE Trans. Power Electron.*, vol.26, no.3, pp.943-952, Mar. 2011.

[10] S. Jiang, D. Cao, Y. Li, J. Liu, and F.Z. Peng, "Low-THD, fast-transient, and cost-effective synchronous-frame repetitive controller for three-phase UPS inverters," *, IEEE Trans. Power Electron.*, vol.27, no.6, pp.2994-3005, Jun. 2012.

[11] K. Zhou, D.W. Wang, B. Zhang, and Y. Wang, "Plug-in dual-mode-structure repetitive controller for CVCF PWM inverters," *IEEE Trans. Power Electron.*, vol.19, no.4. pp.1060-1067, Jul., 2004.

[12] Z. Zou, Z. Wang, M. Cheng, and Y. Yang, "Active power filter for harmonic compensation using a digital dual-mode-structure repetitive control approach," in *Proc. of PEDG'12*, pp.161-166, 25-28 Jun. 2012.

[13] M. Saitou and T. Shimizu, "Generalized theory of instantaneous active and reactive powers in single-phase circuits based on hilbert transform", in *Proc. of PESC'02*, vol. 3, pp. 1419‑1424, 2002.

[14] R. I. Bojoi, L.R. Limongi, D. Roiu, and A. Tenconi, "Enhanced power quality control strategy for single-phase inverters in distributed generation systems," *IEEE Trans. Power Electron.*, vol. 26, no.3 pp. 798-806, 2011.

[15] B. Zhang, D. Wang, K. Zhou, and Y. Wang, "Linear phase lead compensation repetitive control of a CVCF PWM inverter," *IEEE Trans. Ind. Electron..*, vol.55, no.4, pp,1595-1602, 2008.

[16] Y. Cho, and J. Lai, "Digital plug-in repetitive controller for single-phase bridgeless PFC converters," *IEEE Trans. Power Electron.*, vol.28, no.1, pp.165-175, Jan. 2013.

[17] D. Chen, J. Zhang, and Z. Qian, "An improved repetitive control scheme for grid-connected inverter with frequency-adaptive capability," *IEEE Trans. Ind. Electron.*, vol.60, no.2, pp.814-823, Feb. 2013.

[18] R. Costa-Castello, R. Grino, and E. Fossas, "Odd-harmonic digital repetitive control of a single-phase current active filter," *IEEE Trans. Power Electron.*, vol.19, no.4, pp. 1060- 1068, Jul. 2004.

[19] Y. Yang, K. Zhou, and M. Cheng, "Phase compensation resonant controller for single-phase PWM converters," *, IEEE Trans. Ind. Inform.*, forth-coming, 2013.

[20] K. Zhang, Y, Kang, J. Xiong, and J. Chen, "Direct repetitive control of SPWM inverter for UPS purpose," *IEEE Trans. Power Electron.*, vol.18, no.3, pp. 784- 792, May 2003.

[21] M. Castilla, J. Miret, J. Matas, L. Garcia de Vicuna, and J. M. Guerrero, "Control design guidelines for single-phase grid-connected photovoltaic inverters with damped resonant harmonic compensators," *IEEE Trans. Ind. Electron.*, vol.56, no.11, pp.4492-4501, Nov. 2009.

[22] G. Shen, X. Zhu, J. Zhang, and D. Xu, "A new feedback method for PR current control of LCL-filter-based grid-connected inverter," *IEEE Trans. Ind. Electron.*, vol.57, no.6, pp.2033-2041, Jun. 2010.

[23] M. Rashed, C. Klumpner, and G. Asher, "Control scheme for a single phase hybrid multilevel converter using repetitive and resonant control approaches," in *Proc. of EPE'11*, pp.1-13, Aug. 30-Sept. 1 2011.

[24] M. Prodanovic, K. De Brabandere, J. Van Den Keybus, T. Green, and J. Driesen, "Harmonic and reactive power compensation as ancillary services in inverter-based distributed generation," *IET Gener., Transm., Distrib.*, vol.1, no.3, pp.432-438, May 2007.

[25] M. Ciobotaru, R. Teodorescu, and F. Blaabjerg, "Control of single-stage single-phase PV inverter," in *Proc. of EPE'05*, pp.P.1-P.10, 2005.

[26] E. ON GmbH, "Grid Code - High and Extra High Voltage." [Online]. Available: http://www.eon-netz.com/.